Cell, Vol. 86, 767–775, September 6, 1996, Copyright ©1996 by Cell Press

Solution Structure of the Link Module: A Hyaluronan-Binding Domain Involved in Extracellular Matrix Stability and Cell Migration

Daisuke Kohda,*§ Craig J. Morton,† Ashfaq A. Parkar,* Hideki Hatanaka,‡ Fuyuhiko M. Inagaki,‡ Iain D. Campbell,*† and Anthony J. Day*

*Department of Biochemistry
†Oxford Centre for Molecular Sciences
University of Oxford
South Parks Road
Oxford OX1 3QU
United Kingdom
‡Tokyo Metropolitan Institute of Medical Science
Honkomagome 3-chome
Bunkyo-ku
Tokyo 113
Japan

Summary

Link modules are hyaluronan-binding domains found in proteins involved in the assembly of extracellular matrix, cell adhesion, and migration. The solution structure of the Link module from human TSG-6 was determined and found to consist of two α helices and two antiparallel β sheets arranged around a large hydrophobic core. This defines the consensus fold for the Link module superfamily, which includes CD44, cartilage link protein, and aggrecan. The TSG-6 Link module was shown to interact with hyaluronan, and a putative binding surface was identified on the structure. A structural database search revealed close similarity between the Link module and the C-type lectin domain, with the predicted hyaluronan-binding site at an analogous position to the carbohydrate-binding pocket in E-selectin.

Introduction

Interactions between the ubiquitous glycosaminoglycan, hyaluronan (HA), and HA-binding proteins are crucial for the formation and stability of the extracellular matrix as well as many aspects of cell behavior during development, morphogenesis, tumorigenesis, and inflammation (see Knudson and Knudson, 1993; Neame and Barry, 1993; Sherman et al., 1994). The HA interactions are often mediated by a common protein domain termed a Link module, also known as a proteoglycan tandem repeat (Perkins et al., 1989; Hardingham and Fosang, 1992; Bork and Bairoch, 1995). This module is approximately 100 amino acids in length and has a characteristic consensus sequence, containing four disulfide-bonded cysteines (Neame et al., 1986; Neame and Barry, 1993). Link modules have been described in extracellular matrix molecules (link protein, aggrecan, versican, neurocan, and brevican), the HA receptor CD44, and the arthritis-associated protein tumor necrosis factor (TNF)-stimulated gene-6 (TSG-6). The widespread use of the Link module in HA binding is illustrated below with a brief description of its role in cartilage formation and inflammation.

Link protein is an essential constituent of cartilage extracellular matrix and, together with HA and the proteoglycan aggrecan, forms large multimolecular aggregates that provide the tissue with its capacity to bear load and resist deformation (Neame and Barry, 1993). Link protein also occurs in many noncartilaginous tissues, where it stabilizes proteoglycan binding to HA (Binette et al., 1994). Electron microscopy has revealed that a dense array of alternating aggrecan and link protein molecules form along a central HA filament (Morgelin et al., 1988, 1995). Link protein is comprised of an N-terminal immunoglobulin module followed by two Link modules (Neame et al., 1986) that can both bind independently to HA (Grover and Roughley, 1994; Varelas et al., 1995). A homologous N-terminal proteolytic fragment of aggrecan, termed the G1 domain (Doege et al., 1987), is responsible for binding to both link protein and HA (Morgelin et al., 1988; Fosang et al., 1990). An equivalent region is also found in the aggrecan-related proteoglycans versican, neurocan, and brevican, which are expressed in the central nervous system and brain (Zimmermann and Ruoslahti, 1989; Rauch et al., 1992; Yamada et al., 1994).

The cell surface molecule CD44 has a single N-terminal Link module (Goldstein et al., 1989; Haynes et al., 1989) that is involved in HA binding (Peach et al., 1993). CD44 on cartilage chondrocytes is involved both in the assembly of the pericellular matrix, by binding to HA in coordination with proteoglycans, and in the local turnover of HA by endocytosis (Knudson and Knudson, 1993). CD44 also has proinflammatory functions, being up-regulated on many synovial cell types in patients with arthritis (Haynes et al., 1991). In murine models of arthritis, CD44 mediates the migration of inflammatory leukocytes into the extravascular compartment of the synovium by HA binding (Mikecz et al., 1995). In this regard, the rolling of lymphocytes on vascular endothelium has recently been found to occur via the interaction of CD44 with HA (DeGrendele et al., 1996).

Human TSG-6 was first cloned from a cDNA library prepared from TNF-treated FS-4 fibroblasts and contains a Link and a CUB module as shown in Figure 1 (Lee et al., 1992). There is no constitutive expression in fibroblasts, chondrocytes, or synovial cells, but rapid onset of transcription, and subsequent secretion of the gene product, is seen after treatment with interleukin-1 or TNF (see Maier et al., 1996). TSG-6 protein has been detected in the synovial fluids from individuals with arthritis, but is not present in normals, and it was found to be constitutively expressed in synoviocytes from a rheumatoid arthritis patient (Wisniewski et al., 1993). It thus seems likely that TSG-6 is produced locally in inflamed joints and may serve as a useful marker in arthritis. Recombinant TSG-6 coprecipitates with HA in the presence of cationic detergent and is, therefore,

§ Present address: Nuclear Magnetic Resonance Group, Biomolecular Engineering Research Institute, Furuedai 6-chome, Suita, Osaka 565, Japan.

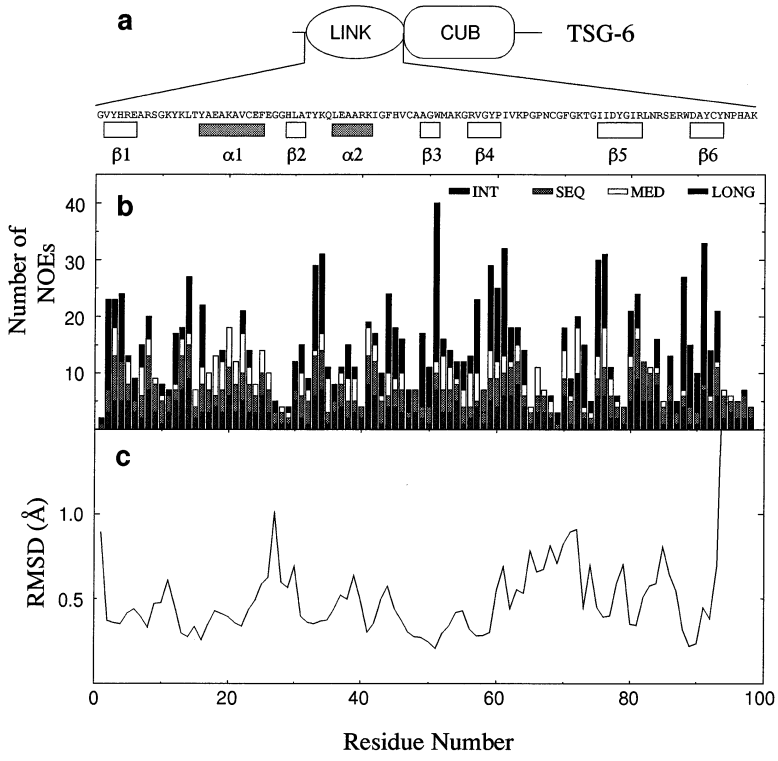

Figure 1. Sequence and Structural Characteristics for the Link Module from Human TSG-6

(a) Schematic diagram showing the sequence of the recombinant Link module within the context of the domain organization of TSG-6, along with the determined secondary structure.

(b) Histogram showing the number of intraresidue (INT), sequential ($|i-j| = 1$; SEQ), medium-range ($2 \leq |i-j| \leq 5$; MED), and long-range ($|i-j| \geq 6$; LONG) NOEs per residue used in the structure calculations. Rmsd from all distance constraints (875) and from experimental ϕ dihedral angle restraints (19) are 0.100 ± 0.0018 Å and 2.54 ± 1.10°, respectively.

(c) Histogram of the atomic rmsd from the mean atomic position for each residue in the 20 selected structures. Residues 94–98 have rmsds greater than 1.5 Å.

likely to be an HA-binding protein, potentially via its Link module. It has been suggested that TSG-6 might be involved in the destabilization of HA–proteoglycan complexes at sites of inflammation (Lee et al., 1992), but a recent report indicates that it may have an anti-inflammatory role (Wisniewski et al., 1996).

The Link module is thus clearly involved in a variety of important functions related to HA binding, yet nothing is known about the structural basis of this activity. We have produced the Link module from TSG-6 (referred to here as residues 1–98; see Figure 1) by expression in Escherichia coli, as described previously (Day et al., 1996). The expressed polypeptide was shown to bind HA, and its 3-dimensional structure was determined in solution by nuclear magnetic resonance (NMR) spectroscopy. The TSG-6 Link module structure, which defines the consensus fold for this module superfamily, was unexpectedly found to have structural similarity to other protein domains that bind carbohydrate.

Results and Discussion

Structure of the TSG-6 Link Module

The structure determination of the TSG-6 Link module was based on a total of 875 nuclear Overhauser effect (NOE)-derived interproton distance, and 19 ϕ dihedral angle, restraints obtained from spectra collected at pH 6.0 (see Experimental Procedures). A total of 200 structures were calculated, and of these the 20 lowest energy structures were selected. Figure 1 shows the number of NOEs per residue, which correlates well with the root-mean-square deviation (rmsd) from the mean atomic positions. As illustrated in Figure 2a, only the N- and C-termini of the module (residues 1 and 94–98, respectively) are disordered. For residues 2–93, the rmsd from the mean structure is 0.54 ± 0.09 Å for the Cα, C, and N atoms, indicating that the backbone of the Link module is well defined. The core of the molecule is also well defined, with an rmsd of 0.99 ± 0.11 Å, from the average coordinates, for all heavy atoms. This is illustrated in Figure 2b, which shows an overlay of the disulfide bonds and selected hydrophobic core residues from the family of structures superimposed on the mean backbone.

The structure, which has a compact fold with a somewhat flattened shape, contains two α helices and two antiparallel β sheets, as shown in Figure 3. The position of these secondary structure elements in relation to the Link module sequence is indicated in Figure 1. In the absence of hydrogen exchange data (see Experimental Procedures), elements of secondary structure were defined on the basis of NOE connectivities. Sheet I (SI) is composed of three strands: β1 (residues 2–6); β2 (residues 29–31); and β6 (residues 89–93). The short strand β2 pairs almost perpendicularly with β6. The two peripheral strands of SI, β1 and β2, are connected by a turn (residues 8–11) similar to a type II turn (Wilmot and Thornton, 1988) and a 10 residue helix (α1, residues 16–25), whereas the central β6 strand is linked to the α1 helix by a disulfide bond (Cys-23–Cys-92). The α1 helix has a typical N-terminal capping sequence (Thr-15 and Glu-18) and a C-terminal, glycine-based (Gly-27 and Gly-28) Schellman motif (Harper and Rose, 1993; Aurora et al., 1994). The other antiparallel β sheet (SII) is also composed of three strands (β3, residues 49–51; β4, 56–60; β5, 75–81) where the β5 strand contains a bulge (77–79). Sheet SI is in contact with SII via the

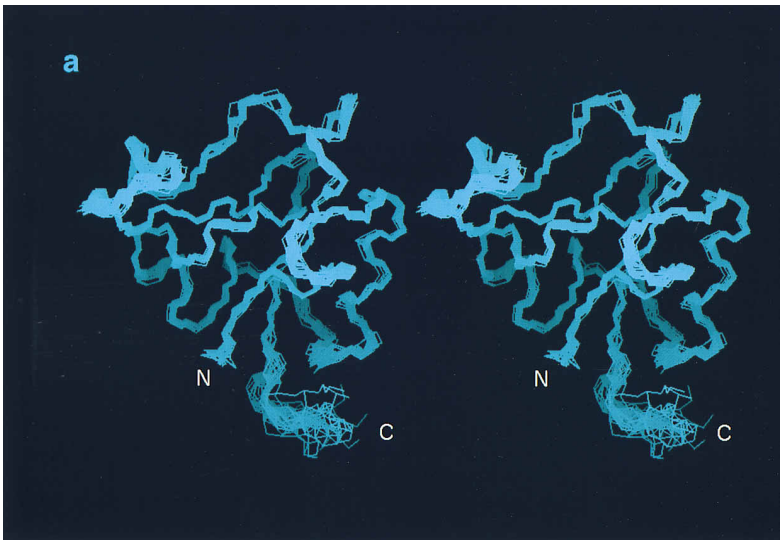

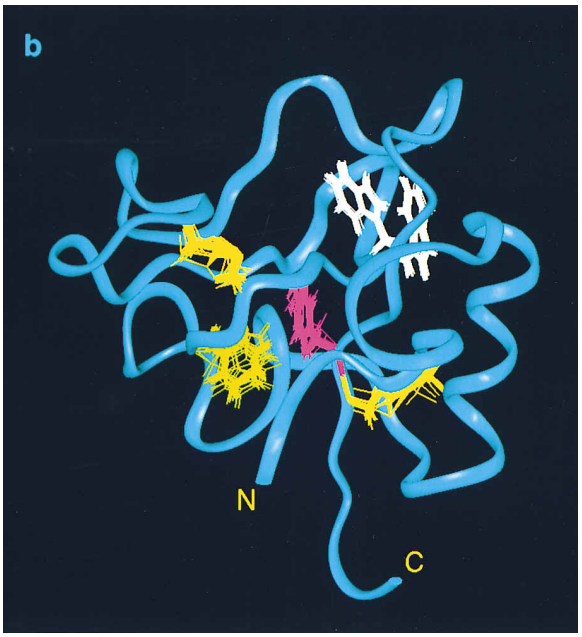

Figure 2. Overlay of the 20 Final Structures on the Average Coordinate Position for the Backbone Atoms of Residues 2–93

(a) Stereoview of backbone traces for the family of structures.

(b) Side chain traces of aromatic hydrophobic core residues (Phe-44 in green, Trp-51 and Trp-88 in white, and Tyr-91 in pink) and disulfide bonds (Cys-23 to Cys-92 and Cys-47 to Cys-68 in yellow) where the mean structure is shown by a blue ribbon.

formation of a parallel β-sheet structure, pairing residues 50 and 51 of β3 with 89 and 90 of β6. The six residue α2 helix (36–41) lies in a loop, between β2 and β3. The irregular segment (42–48) following this helix is linked, by the Cys-47–Cys-68 disulfide, to the long loop (61–74) between β4 and β5 that is rich in glycine and proline.

The TSG-6 Link module has a large and well-defined hydrophobic core composed of side chains from 21 amino acids, including the disulfide bond between Cys-23 and Cys-92 (see Figure 4). The majority of these residues are located either in the SII sheet (β3, Ala-49, Gly-50, Trp-51; β4, Val-57, Gly-58, Pro-60; β5, Ile-75, Ile-76, Ile-80) or in the β6 strand (Asp-89, Ala-90, Tyr-91, Cys-92). Strands β3 and β6 have a particularly important role in stabilizing the structure and provide much of the central scaffold. Figure 2b shows the contribution of aromatic residues to the core, where the two tryptophans (51 and 88) lie very close together. In a 1-dimensional NMR spectrum, methyl protons are seen at −0.532 and −1.089 ppm (Day et al., 1996). These come from Val-57 (β4) where the protons are shifted to high field owing to close contact with Trp-51 (β3) and Trp-88 (β6). We note that Asp-89 in β6 is completely buried within the protein and is likely to have a high pK_a. This amino acid may form hydrogen bonds with the backbone amide protons of amino acids 11–13 and thus be involved in restraining the region between β1 and α1 (residues 7–15).

The N- and C-termini of the Link module are close to each other in such a way that Val-2 and Tyr-93 are adjacent residues and define the boundaries of the structural domain (see Figures 1 and 2). The N-terminal and the five C-terminal residues are not well-resolved in the structure and, therefore, are probably domain-connecting peptides. The novel structure reported here defines the global fold for this module type.

Comparison with Other Link Modules

Figure 4 also shows a comparison of the amino acid sequences of the TSG-6 Link module with those from human CD44, cartilage link protein, and the G1 domain of aggrecan, in which the level of sequence identity ranges from 32.3% (CD44 and LK-2) to 37.9% (AG-1). From this alignment it can be seen that the residues that define the hydrophobic core in TSG-6, including the amino acids of the β3 and β6 sheets, are highly conserved in these proteins. There are no insertions or deletions present in regions corresponding to elements of the secondary structure, and those that do occur would mainly affect the length of exposed loops. Possible exceptions are a seven amino acid insertion and a three residue deletion, at the position of the bulge in the β5 strand, in the second Link module of aggrecan (AG-2) and CD44, respectively. In AG-2, this insertion is expected to be accommodated as an additional loop within the structure, whereas the absence of a bulge in CD44 may cause local structural modification to the

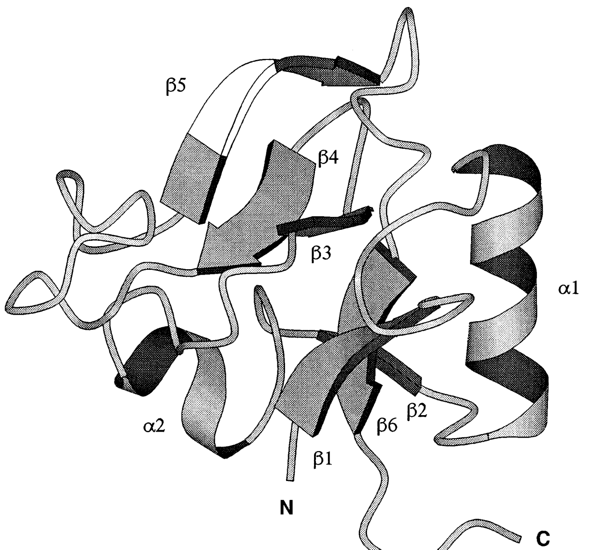

Figure 3. The Secondary Structure Organization of the Link Module, Which Consists of Two Helices (α1 and α2) and Two Antiparallel β Sheets

The SI sheet is composed of strands β1, β2, and β6 and the SII sheet of β3, β4, and β5. The β5 strand contains a bulge (residues 77–79), which is indicated by no shading. This figure, in which the structure is in the same orientation as in Figure 2, was made using the program MOLSCRIPT (Kraulis, 1991).

length or position of the β5 strand (relative to β4). Therefore, the Link module from TSG-6 is typical of Link modules in general, and our structure will allow useful modeling of other superfamily members.

HA Binding of the TSG-6 Link Module

Recombinant full-length TSG-6 has been demonstrated previously to interact with HA (Lee et al., 1992). An HA binding assay was developed to investigate whether the expressed Link module of TSG-6, used in structure determination, mediates this interaction (see Experimental Procedures). In this assay, the binding of biotinylated HA (bHA) to a Link module–coated plate was measured colorimetrically using a 250 kDa fragment of HA modified to give biotinylation of about 1 in 50 of the carboxyl moieties. A similar probe has been used recently to detect the presence of HA-binding proteins on blots and in tissue slices (Yu and Toole, 1995). Figure 5a shows that the TSG-6 Link module does indeed bind to HA. There was close to maximum binding of bHA when 25 pmol (~0.3 μg) of the Link module was coated per well. Therefore, this amount of protein was used in the subsequent competition assay. In Figure 5b, it can be seen that the binding of bHA could be almost fully competed by unlabeled HA. The G1 domain of aggrecan, a well-characterized HA-binding domain (Fosang et al., 1990) that contains two Link modules, was found to bind bHA in a similar manner, indicating that the assay is reliable (see Figure 5b). Therefore, the recombinant Link module of TSG-6 interacts specifically with HA. These experiments were performed at a pH (5.8) at which the protein has been shown by NMR to be fully folded (data not shown).

Identification of a Putative HA-Binding Surface

Visual inspection of the Link module structure revealed the presence of a solvent-exposed hydrophobic patch made up of Tyr-12, Tyr-59, Tyr-78, and part of Trp-88 (see Figure 6). Hydrophobic amino acids are highly conserved at these positions in CD44, cartilage link protein, and aggrecan (see Figure 4). Similar amino acids have been found to have important roles in protein–carbohydrate interactions, e.g., by making hydrophobic contacts with the C-5 and C-6 carbons of hexopyranoside rings (Vyas, 1991; Sharon, 1993). Positively and negatively charged amino acids (Lys-11, Lys-72, Asp-77, Arg-81, and Glu-86) are arranged around this patch (see Figure 6). Arginine and lysine residues have been implicated in HA binding by chemical modification studies on cartilage link protein (Lyon, 1986) and aggrecan (Hardingham et al., 1976), where these are likely to form ionic interactions with the carboxylate anions of HA (Christner et al., 1977). In light of these data, the hydrophobic/hydrophilic region of the Link module could be involved in HA binding. Similar patches are likely to be formed in the other members of the Link module superfamily, as there is conservation of the hydrophobic and some of the charged residues. As can be seen from

```
              10        20        30        40         50        60        70                  80        90
               :         :         :         :          :         :         :                   :         :
CD44  GVFHVE KNGrYSISRTEAADLCKAFNSTLPTMAQMEKALSI GFETCRYGFI EGHVVIPRIHPNSICAANN   TGVY          ILTSNTSQYDTYCFNASAP
LK-1  VVFPYFPRLGRYNLNFHEAQQACLDQDAVIASFDQLYDAWRG GLDWCNAGWLSDGSVQYPITKPREPCGGQN TVPGVRNY       GFWDKDKSRYDVFCFTSNFN
LK-2  GRFYYLIHPTKL  TYDEAVQACLNDGAQIAKVGQIFAAWKILGYDRCDAGWLADGSVRYPISRPRRRCSPTE   AAVRFV       GFPDKKHKLYGVYCFRAYN
AG-1  IVFHYRAISTRYTLDFDRAQRACLQNSAIIATPEQLQAAYED GFHQCDAGWLADQTVRYPIHTPREGCYGDKDEFPGVRTY       GIRDT NETYDVYCFAEEME
AG-2  EVFYAT SPEKF  TFQEAANECRRLGARLATTGHVYLAWQA GMDMCSAGWLADRSVRYPISKARPNCGGNL   LGVRTVYVHANQTGYPDP SSRYDAICYTGEDF
TSG6  GVYHREARSGKYKLTYAEAKAVCEFEGGHLATYKQLEAARKI GFHVCAAGWMAKGRVGYPIVKPGPNCGFGK   TGIIDY       GIRLNRSERWDAYCYNPHAK
                ♦♦                                               ♦            ♦       ♦♦         ♦    ♦ ♦
CON    VF       +¥   π EA  øC      øAt  Qø  A¥   G¥  C ¥Gπø -  V ¥PI  P   C        Gø  ¥       G¥       πDø¥Cπ
SS     bbbbb         aaaaaaaaaa    bbb   aaaaaa         bbb   bbbbb                 bb^^       ^bb      bbbbb
```

Figure 4. Multiple Sequence Alignment of the Link Module Superfamily

Sequence alignment of the TSG-6 Link module with those from CD44, cartilage link protein (LK-1 and LK-2), and the G1 domain of aggrecan (AG-1 and AG-2). All the sequences are from human proteins and taken from GenBank (HUMCD44B, HSLINKC, and HUMAGPRO). The alignment was generated using the program AMPS (Barton and Sternberg, 1987), and minor adjustments were made manually. For the TSG-6 Link module amino acid numbering, secondary structure (SS) elements (a, α helix; b, β strand; caret indicates the bulge in β5) and core residues (black background) are shown. The consensus sequence (CON) indicates the presence of identical amino acids (one-letter code) or conservative replacements (plus: K or R; minus: D or E; t: S or T; π: aromatics F, Y, or W; ϕ: aliphatic hydrophobics A, M, I, L, or V; ¥: π or ϕ) in at least five of the sequences as indicated by the gray background. Regions implicated in HA binding are underlined, and the residue R-41 in CD44 is shown in lower case. Amino acids that form the putative HA-binding surface in TSG-6 are denoted by closed diamonds. On the basis of this alignment, the TSG-6 Link module (residues 1–93) has 32.3% identity with CD44, 33.7% with LK-1, 32.3% with LK-2, 37.9% with AG-1, and 35.4% with AG-2.

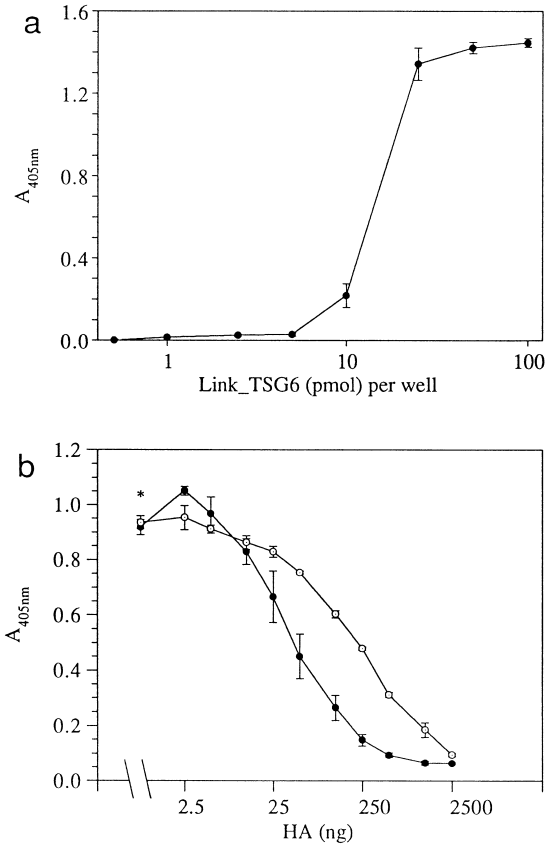

Figure 5. HA Binding Assay

(a) bHA binding, at pH 5.8, to different amounts of TSG-6 Link module (Link_TSG-6) coated onto wells of a microtiter plate. The level of bHA binding (A_{405nm}) was measured following color development. Values are plotted as mean absorbance (n = 3) ± standard error of the mean (SEM).

(b) Link_TSG-6 (25 pmol per well; closed circles) or G1 domain of aggrecan (25 pmol per well; open circles) were coated on separate plates, and bHA binding at pH 5.8 was measured in the absence (asterisk) or presence of competing unlabeled HA. Values are plotted as mean absorbance (n = 4) ± SEM.

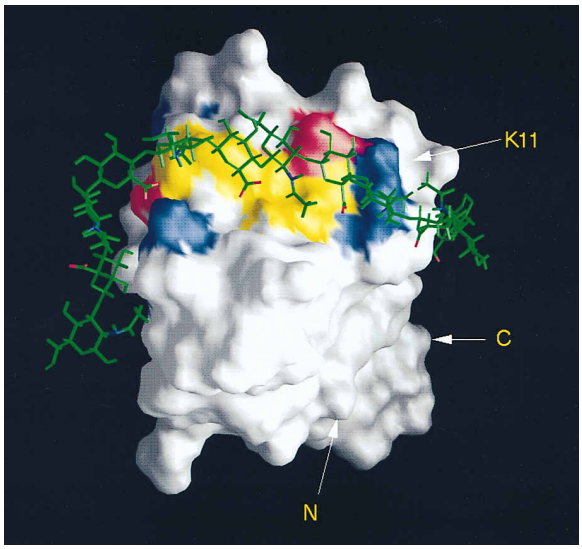

Figure 6. Putative HA-Binding Surface of Link Module

The solvent-accessible surface of the protein is shown, where residues that comprise the predicted HA-binding site are highlighted: aromatics in yellow (Tyr-12, Tyr-59, Tyr-78, and Trp-88), basics in blue (Lys-11, Lys-72, and Arg-81), and acidic residues in red (Asp-77 and Glu-86). The HA_{12}, i.e., six [D-glucuronic acid (β1→3) N-acetyl-D-glucosamine (β1→4)] disaccharide units, is shown in green, with the carboxyl oxygens of D-glucuronic acid and the nitrogen atom of N-acetyl-D-glucosamine in red and blue, respectively. The N- and C-termini and Lys-11 of the protein are indicated. From the figure it can be seen that, if a single Link module does interact with an HA_{10}, then contacts could occur with regions of the protein outside the predicted binding surface.

Figure 4, the amino acids that form this surface are brought together from different parts of the sequence. Interestingly, most of these amino acids come from regions of the Link module that have been previously implicated in HA binding of cartilage link protein or CD44 (Goetinck et al., 1987; Yang et al., 1994; Zheng et al., 1995). Furthermore, Peach et al. (1993) have demonstrated that mutation of the conserved Arg-41 of CD44 (equivalent to Lys-11 in our structure) to alanine completely abolishes HA binding. This basic amino acid is located next to one of the surface-exposed hydrophobic residues (Tyr-12) on the 7–15 loop between β1 and α1. Therefore, this loop region may be of particular functional importance. As noted above, the buried Asp-89 (in its protonated state) may have a role in restraining this loop. This amino acid is conserved in CD44, AG-1, AG-2, and LK-1, but is replaced by a glycine in LK-2, as shown in Figure 4. It is possible that the nature of the amino acid residue at this position will determine the pH dependencies of HA binding by these proteins.

It is well established that a decasaccharide (i.e., HA_{10}) is the minimum size of HA that can interact strongly with aggrecan or link protein (Hardingham and Muir, 1973; Hascall and Heinegård, 1974). These proteins each contain two Link modules which, in Link protein at least, can both interact with HA (Grover and Roughley, 1994). To our knowledge, the size of HA oligomer that interacts with an individual module in these proteins has not been studied directly. However, CD44, which contains a single Link module, binds to an HA_6 (Underhill et al., 1983). In TSG-6, which also contains a single Link module, the size of carbohydrate ligand has not yet been established. Figure 6 shows a speculative model of how an HA_{12} could dock on the putative HA-binding site discussed above. Work is in progress in our laboratory to define this binding site experimentally.

Comparison of the Link Module with Other Structures

An automated search of the DALI database (Holm et al., 1992; Holm and Sander, 1994) revealed an unexpected similarity between the Link module structure and the C-type lectin domain of human mannose-binding protein C-chain (MBP-C; Sheriff et al., 1994). An overlay of these structures is shown in Figure 7. These domains have identical topologies and a very similar organization of secondary structure with an rmsd of 2.89 Å for backbone atoms of 70 structurally equivalent residues. We

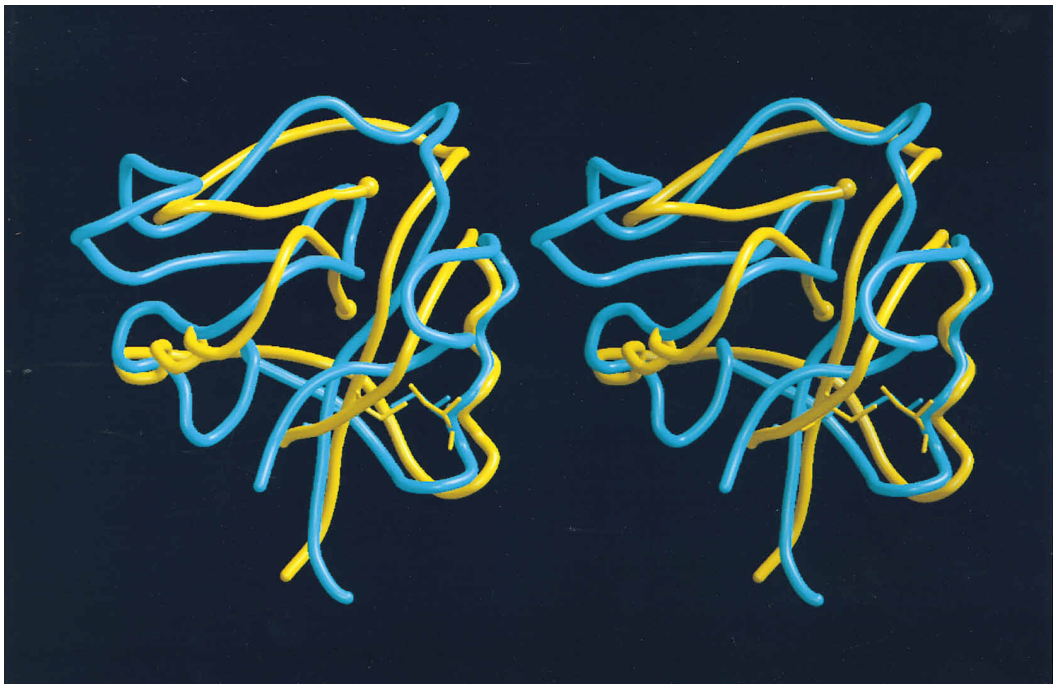

Figure 7. A Comparison of the Structures of the Link Module and the C-Type Lectin Domain

A stereoview showing the Link module in blue and the C-type lectin domain in yellow. Residues 1–96 of the Link module are overlaid with residues 119–228 of the human MBP-C (Sheriff et al., 1994) on the basis of structurally equivalent residues determined by a search of the DALI database (Holm et al., 1992; Holm and Sander, 1994) with the Link module mean coordinates. The equivalent disulfide bonds in the Link module (Cys-23 to Cys-92) and in the C-type lectin (Cys-135 to Cys-224) are shown. The long calcium-binding loop of the C-type lectin, residues 166–201, is not displayed for the sake of clarity. This region has no equivalent in the Link module. Residues 165 and 202, the points where this loop enters and leaves the structure, are indicated on the figure by small spheres. The coordinates of the C-type lectin domain were obtained from the Brookhaven Protein Data Bank (entry 1HUP).

note that the interstrand hydrogen bond network is similar in the two structures. The major differences between the structures is the length of two loops. The long loop (residues 166–201 in MBP-C), which contains Ca^{2+}-binding residues in the lectin domain (Weis et al., 1991), is absent from the Link module. At this position the Link module has a much shorter loop (residues 53–55) between the β3 and β4 strands (see Figure 4). Similarly, the loop between β4 and β5 (residues 62–74) in the Link module is shorter in the lectin domain. The interiors of the structures are also quite similar, with conservative replacements found in the lectin domain, at equivalent sequence positions, for 13 of the 21 core residues in the Link module. This includes the disulfide bond between Cys-23 and Cys-92 in the Link module (Cys-135 to Cys-224 in the lectin domain). These structural similarities between the Link module and the lectin domain suggest that they have a common evolutionary origin, even though the overall sequence similarity is below the level of statistical significance. This is intriguing given that both of these structures are involved in carbohydrate recognition.

Recently, the N-terminal regions of the S2 and S3 subunits of pertussis toxin, from the whooping cough bacteria Bordetella pertussis, have been found to be structurally related to the C-type lectin domain (Stein et al., 1994). The S2 and S3 structures have an identical topology to the Link module with a similar organization of secondary structure, where only the β1 strand and α1 helix are missing (data not shown). Like the Link module, they do not contain a long Ca^{2+}-binding loop. At the sequence level, there is no significant similarity to either the Link module or lectin domain, but there are a number of residues in equivalent core positions, including a disulfide bond.

In the C-type lectin domain of MBP, the residues that bind Ca^{2+} ions are also largely responsible for carbohydrate binding (Weis et al., 1992). These amino acids are mostly located in the long loop (residues 166–201 in MBP-C), which is absent in the Link module (see above). Since there is no evidence that HA binding is Ca^{2+} dependent, it is perhaps not surprising that the Link module lacks this region. However, Asp-77 and Tyr-78 in the putative Link module HA-binding site are in similar positions (on the β5 strand) to other calcium-chelating residues in MBP (Asn-212 and Asp-213 in human MBP-C). In the lectin domain of E-selectin, although Ca^{2+}-chelating residues are functionally important, a much larger protein surface is involved in carbohydrate binding than in MBP (Graves et al., 1994; Kogan et al., 1995). We note that amino acids of the putative Link module HA-binding surface (Tyr-59, Arg-81, Glu-86, and Trp-88) are in equivalent backbone positions to residues of the sialyl $Lewis^x$ binding site of E-selectin (Tyr-94, Glu-107, Lys-111, and Lys-113, respectively). This is interesting, particularly given the recent finding that CD44 can mediate the rolling of leukocytes on the vascular endothelium by binding to HA (DeGrendele et al., 1996), a process in which

the selectins are also involved (Lawrence and Springer, 1991; Jutila et al., 1994).

Conclusions

We have defined the consensus structure for the Link module, which gives novel molecular insight into the mode of action of a protein superfamily involved in extracellular matrix assembly and cell migration. Identification of a putative HA-binding site on the Link module forms the basis for further investigations to define the exact nature of this important protein–carbohydrate interaction in the arthritis-associated protein TSG-6. The structural similarity between the Link module and the C-type lectin domain suggests that these have a common evolutionary origin, which provides a possible explanation for the similar roles of CD44 and the selectins in leukocyte extravasation at sites of inflammation.

Experimental Procedures

Protein Expression

The Link module corresponds to residues 36–133 in the TSG-6 preprotein (Lee et al., 1992). Cloning and overexpression of this module in E. coli to produce unlabeled and uniformly ^{15}N-labeled samples has been reported previously (Day et al., 1996); the purified proteins were shown to have the expected disulfide bond organization and the correct molecular masses.

NMR Spectroscopy and Structure Calculations

Protein samples (including ^{15}N-enriched samples) were dissolved in either H_2O, containing 10% (v/v) D_2O and 0.02% (w/v) NaN_3, or D_2O (≥99.96% isotopic purity) to a concentration of ~1 mM and were adjusted to the required pH with NaOH or NaOD, respectively. All NMR spectra were recorded using home-built/GE Omega spectrometers operating at proton frequencies of 600 and 750 MHz. FELIX 2.3 (Biosym) was used to process the NMR data, and baseline correction and peak picking were performed with the programs described in Hatanaka et al. (1994).

Homonuclear 2-dimensional ^1H NMR spectra were collected at either pH 5.1 and 37°C or at pH 6.0 and 20°C. In addition, 4 mM $ZnSO_4$ was included in the pH 6.0 samples, as this was found to increase their long-term stability while having little effect on spectral quality. At pH 6.0 and 20°C, high quality NOESY, but relatively poor total correlated spectra (TOCSY), were obtained. The low quality of the TOCSY data was due to some self-association of the protein (A. J. D., unpublished data). At pH 5.1 and 37°C, better TOCSY data were obtained, but the NOESY spectra were overlapped (particularly in the fingerprint region) owing to the presence of both folded and partially unfolded protein in the sample. As neither condition alone gave data of sufficient quality for complete sequential assignment, a combination of NOESY (Jeener et al., 1979; Macura et al., 1981), COSY (Braunschweiler and Ernst, 1983; Bax and Davis, 1985), and TOCSY (Aue et al., 1976; Brown et al., 1988) spectra at both pH 5.1 and pH 6.0 was used.

Semiautomatic assignment of the NOESY spectra, collected at pH 6.0 with a mixing time of 150 ms, was performed with the program XPLOR-UP (Hatanaka et al., 1994) to generate an unbiased set of distance restraints. Ambiguous NOE cross peaks were assigned, in an iterative manner, with reference to calculated preliminary structures, using conservative selection parameters. This analysis was helped by the high proportion of amino acids with simple spin networks (13 glycine and 12 alanine). Peak intensities were transformed into distances on the basis of known distances: sequential $d_{\alpha N}$ β strand = 2.2 Å in ^1H_2O NOESY, and interstrand $d_{\alpha\alpha}$ in antiparallel β sheet = 2.3 Å in ^2H_2O NOESY using the relationship (NOE intensity) ∝ (distance)$^{-a}$. An empirical value of $a = 4$ was used to take account of spin diffusion effects at the mixing time used (Suri and Levy, 1993). The upper bond distance constraints were the calculated distance plus 0.5 Å, and the lower limits were set to 1.8 Å. After 10 cycles of iterative NOESY peak assignment and structure calculation a total of 348 intraresidue (|i-j| = 0), 167 sequential (|i-j| = 1), 109 medium-range (2 ≤ |i-j| ≤ 5), and 251 long-range (|i-j| ≥ 6) (including 2 derived from disulfide bonds) distance restraints were used in the final structure calculations. A ^{15}N–^1H HMQC-J experiment (Kay and Bax, 1990) at pH 6.0 was used to determine ϕ dihedral angles. Slow-exchanging amide protons were not detected, as the protein was dissolved under conditions at which it is completely unfolded (i.e., ~pH 3.5). Consequently, no hydrogen bond restraints were applied during structure calculations.

A total of 200 structures were calculated on the basis of 875 NOE distance and 19 ϕ dihedral angle constraints using the program XPLOR 3.1 (Brünger, 1992). The restraints for the disulfide bridges were included in the bond term just before the cooling stage of the XPLOR protocol. The final values of the experimental terms in the force field used during simulated annealing were F_{NOE} = 1831.0 ± 63.2 kJ mol^{-1}, Fc_{dih} = 9.27 ± 6.66 kJ mol^{-1}, with force constants of 209 kJ mol^{-1} Å^{-2} and 209 kJ mol^{-1} rad^{-2}, respectively. The 20 structures with the lowest residual energy (F_{Repel} + F_{NOE} + Fc_{dih}) were selected, with deviations from idealized covalent geometry of 0.0089 ± 0.0003 Å (bonds), 1.36 ± 0.027° (angles), and 2.07 ± 0.032° (impropers).

The mean structure was obtained by averaging the coordinates of the 20 selected structures and subjecting the resulting coordinates to further restrained minimization. In the mean structure there are two torsion angle violations greater than 5.0° (maximum, 13.8°) and no distance constraint violations greater than 0.51 Å. These violations result from the relatively low number of constraints per residue, which was a consequence of the difficulties encountered in recording the NMR data, relative to the good sampling properties of the structure calculation method (see above). However, the small deviation from idealized bond lengths shows the structure has good covalent geometry. The coordinates of the mean structure have been deposited in the Brookhaven Protein Data Bank (entry 1TSG).

Model Building

An HA_{12} was built and docked manually onto the Link module structure using the program SYBYL (Tripos Associates). To remove van der Waals clashes introduced by the modeling process, the complex (i.e., the Link module and HA_{12}) was subjected to 100 rounds of conjugate gradient minimization using the Tripos force field.

Biotinylation of HA

Highly purified HA with a molecular mass of 250 kDa (Kabi Pharmacia, Sweden), a gift from Dr. Mike Bayliss (Kennedy Institute of Rheumatology, London), was biotinylated by the method of Pouyani and Prestwich (1994). To 100 μl of 5 mg/ml HA in H_2O (i.e., ~1.32 μmol of carboxyl groups), 25 μl of 10 mg/ml adipic dihydrazide (1.43 μmol) was added, and the pH was adjusted to 4.75 with 0.1 M HCl. To this, 5 μmol (9.55 μl of a 100 mg/ml solution) of 1-ethyl-3-[3-(dimethylamino)propyl]carbodiimide was added. The reaction mixture was maintained at pH 4.75 by addition of 0.1 M HCl, and after 2 hr no further rise in pH was seen. The pH was then titrated to 7.0 with 1 M NaOH. The reaction mixture was adjusted to 1 ml, dialyzed exhaustively against H_2O, and then lyophilized. The freeze-dried hydrazido–HA was dissolved in 80 μl of 0.1 M $NaHCO_3$ containing 65 μg (29 nmol) of ImmunoPure sulfo-NHS-biotin (Pierce) and mixed at room temperature for 18 hr. Hydrolyzed biotin that precipitated during the reaction was removed by centrifugation. The supernatant was purified on a 10DG desalting column (Bio-Rad, UK) and equilibrated in H_2O to remove any unreacted biotin, and fractions containing bHA were lyophilized. The preparation was resuspended in 100 μl of H_2O. Using this method, a maximum of 1 in 45 of the carboxyls of HA could be modified with biotin (i.e., each HA molecule should contain less than 15 biotin moieties).

HA Binding Assay

This HA binding assay measures the amount of bHA binding to protein immobilized on a microtiter plate in the absence or presence of competing unlabeled HA. All dilutions, incubations, and washes were performed in 10 mM Na-acetate, 140 mM NaCl, 0.05% (v/v) Tween 20 (pH 5.8) at room temperature unless otherwise stated. Wells of plastic Linbro microtiter plates (ICN, UK) were coated overnight either with 200 μl per well of protein solution in 20 mM Na_2CO_3

(pH 9.6) or with buffer alone. The coating solution was removed and the plates were washed three times. The plates were blocked by incubation for 90 min at 37°C with 1% (w/v) bovine serum albumin, followed by three washes. A 1:10,000 dilution of bHA (see above) was made, and 200 μl of this solution, which either contained no HA or various amounts of HA (2.5–2,500 ng), was added to the wells and incubated for 4 hr. The HA used for competition was from human umbilical cord with average molecular mass of 4.4×10^6 Da (Sigma, UK). The plates were washed three times, and 200 μl of a 1:10,000 dilution of Extra-Avidin alkaline phosphatase (Sigma, UK) was added and incubated for 30 min, followed by three washes. A 1 mg/ml solution of the alkaline phosphate substrate, disodium p-nitrophenyl-phosphate, in 100 mM Tris–HCl, 100 mM NaCl, 5 mM $MgCl_2$ (pH 9.3) (200 μl) was added to all wells and incubated until sufficient color had developed (8–12 min). The absorbance at 405 nm was determined on a microtiter plate reader (MKII Titertek Multiscan Plus). All absorbances were corrected against blank wells, which contained substrate solution alone.

The optimum amount of Link_TSG-6 used in this assay was determined by coating with a range of protein concentrations (0.5–100 pmol per well) and binding bHA in the absence of competitor (Figure 5a). On this basis, 25 pmol per well of Link_TSG-6 (or the G1 domain of aggrecan) was used in the competition assay. The G1 domain of aggrecan, purified from porcine laryngeal cartilage, was provided by Ms. Sarah Howat and Dr. Mike Bayliss (Kennedy Institute of Rheumatology, London).

Acknowledgments

Correspondence should be addressed to A. J. D. We thank Dr. Jonathan Boyd for assistance with NMR measurements and Drs. Kristy Downing and Caroline Milner for critical reading of the manuscript. This work, A. J. D., and A. A. P. were supported by the Arthritis and Rheumatism Council (grants D0067 and D0086). D. K. acknowledges support from the Japan Society for the Promotion of Science. The Oxford Centre for Molecular Sciences is funded by the Biotechnology and Biological Sciences Research Council (BBSRC), the Engineering and Physical Sciences Research Council, and the Medical Research Council. C. J. M. is funded through a Protein Engineering BBSRC LINK project. I. D. C. acknowledges the Wellcome Trust for support.

Received May 20, 1996; revised July 16, 1996.

References

Aue, W.P., Partholdi, E., and Ernst, R.R. (1976). Two-dimensional spectroscopy: application to nuclear magnetic resonance. J. Chem. Phys. *64*, 2229–2246.

Aurora, R., Srinivasan, R., and Rose, G.D. (1994). Rules for α-helix termination by glycine. Science *264*, 1126–1130.

Barton, G.J., and Sternberg, M.J.E. (1987). A strategy for the rapid multiple alignment of protein structures: confidence levels from tertiary structure comparisons. J. Mol. Biol. *198*, 327–337.

Bax, A., and Davis, D.G. (1985). MLEV-17–based two-dimensional homonuclear magnetization transfer spectroscopy. J. Magn. Reson. *65*, 355–360.

Binette, F., Cravers, J., Kahoussie, B., Haudenschild, D., and Goetinck, P.F. (1994). Link protein is ubiquitously expressed in non-cartilaginous tissues where it enhances and stabilises the interaction of proteoglycans with hyaluronic acid. J. Biol. Chem. *269*, 19116–19122.

Bork, P., and Bairoch, A. (1995). Extracellular protein modules. Trends Biochem. Sci. *02* (Suppl.).

Braunschweiler, L., and Ernst, R.R. (1983). Coherence transfer by isotropic mixing: application to protein correlation spectroscopy. J. Magn. Reson. *53*, 531–538.

Brown, S.C., Weber, P.L., and Mueller, L. (1988). Toward complete ^{1}H NMR spectra in proteins. J. Magn. Reson. *77*, 166–169.

Brünger, A.T. (1992). XPLOR (Version 3.1): A System for X-Ray Crystallography and NMR (New Haven, Connecticut: Yale University Press).

Christner, J., Brown, M., and Dziewiatkowski, D.D. (1977). Interaction of cartilage proteoglycans with hyaluronic acid: the role of the hyaluronic acid carboxyl groups. Biochem. J. *167*, 711–716.

Day, A.J., Aplin, R.T., and Willis, A.C. (1996). Overexpression, purification and refolding of Link module from human TSG-6 in *Escherichia coli*: effect of temperature, media and mutagenesis on lysine misincorporation at arginine AGA codons. Protein Expr. Purif. *8*, 1–16.

DeGrendele, H.C., Estess, P., Picker, L.J., and Siegelman, M.H. (1996). CD44 and its ligand hyaluronate mediate rolling under physiologic flow: a novel lymphocyte-endothelial cell primary adhesion pathway. J. Exp. Med. *183*, 1119–1130.

Doege, K., Sasaki, M., Horigan, E., Hassel, J.R., and Yamada, Y. (1987). Complete primary structure of the rat cartilage proteoglycan core protein deduced from cDNA clones. J. Biol. Chem. *262*, 17757–17767.

Fosang, A.J., Hey, N.J., Carney, S.L., and Hardingham, T.E. (1990). An Elisa plate based assay for hyaluronan using biotinylated proteoglycan G1 domain (HA-binding region). Matrix *10*, 306–313.

Goetinck, P.F., Stirpe, N.S., Tsonis, P.A., and Carlone, D. (1987). The tandemly repeated sequences of cartilage link protein contain sites for interaction with hyaluronic acid. J. Cell Biol. *105*, 2403–2408.

Goldstein, L.A., Zhou, D.F.H., Picker, L.J., Minty, C.N., Bargatze, R.F., Ding, J.F., and Butcher, E.C. (1989). A human lymphocyte homing receptor, the hermes antigen, is related to cartilage proteoglycan core and link proteins. Cell *56*, 1063–1072.

Graves, B.J., Crowther, R.L., Chandram, C., Rumberger, J.M., Li, S., Huang, K.-S., Presky, D.H., Familletti, P.C., Wolitzky, B.A., and Burns, D.K. (1994). Insight into E-selectin/ligand interaction from the crystal structure and mutagenesis of the lec/EGF domains. Nature *367*, 532–538.

Grover, J., and Roughley, P.J. (1994). The expression of functional Link protein in a baculovirus system: analysis of mutants lacking the A, B and B′ domains. Biochem. J. *300*, 317–324.

Hardingham, T.E., and Fosang, A.J. (1992). Proteoglycans: many forms and functions. FASEB J. *6*, 861–870.

Hardingham, T.E., and Muir, H. (1973). Binding of oligosaccharides of hyaluronic acid to proteoglycans. Biochem. J. *135*, 905–908.

Hardingham, T.E., Ewins, R.J.F., and Muir, H. (1976). Cartilage proteoglycans: structure and heterogeneity of the core protein and the effects of specific protein modification on the binding to hyaluronate. Biochem. J. *157*, 127–143.

Harper, E.T., and Rose, G.D. (1993). Helix stop signals in proteins and peptides: the capping box. Biochemistry *32*, 7605–7609.

Hascall, V.C., and Heinegård, D. (1974). Aggregation of cartilage proteoglycans: oligosaccharide competitors of the proteoglycan-hyaluronic acid interaction. J. Biol. Chem. *249*, 4242–4249.

Hatanaka, H., Oka, M., Kohda, D., Tate, S., Suda, A., Tamiya, N., and Inagaki, F. (1994). Tertiary structure of erabutoxin b in aqueous solution as elucidated by two-dimensional nuclear magnetic resonance. J. Mol. Biol. *240*, 155–166.

Haynes, B.F., Telen, M.J., Hale, L.P., and Denning, S.M. (1989). CD44: a molecule involved in leukocyte adherence and T-cell activation. Immunol. Today *10*, 423–428.

Haynes, B.F., Hale, L.P., Patton, K.L., Martin, M.E., and McCallum, R.M. (1991). Measurement of an adhesion molecule as an indicator of inflammatory disease activity: up regulation of the receptor for hyaluronate (CD44) in rheumatoid arthritis. Arthritis Rheum. *34*, 1434–1443.

Holm, L., and Sander, C. (1994). The FSSP database of structurally aligned protein fold families. Nucl. Acids Res. *22*, 3600–3609.

Holm, L., Ouzounis, C., Sander, C., Tuparev, G., and Vriend, G. (1992). A database of protein structure families with common folding motifs. Protein Sci. *1*, 1691–1698.

Jeener, J., Meier, B.H., Backmann, P., and Ernst, R.R. (1979). Investigation of exchange processes by two-dimensional NMR spectroscopy. J. Chem. Phys. *71*, 4546–4553.

Jutila, M.A., Bargatze, R.F., Kurk, S., Warnock, R.A., Ehsani, N., Watson, S.R., and Walcheck, B. (1994). Cell surface P- and E-selectin support shear-dependent rolling of bovine γ/δ T cells. J. Immunol. *153*, 3917–3928.

Kay, L.A., and Bax, A. (1990). New methods for the measurement of NH-C-α-H coupling constants in N-15 labelled proteins. J. Magn. Reson. *86*, 110–126.

Knudson, C.B., and Knudson, W. (1993). Hyaluronan-binding proteins in development, tissue homeostasis and disease. FASEB J. *7*, 1233–1241.

Kogan, T.P., Revelle, B.M., Tapp, S., Scott, D., and Beck, P.J. (1995). A single amino acid residue can determine the ligand specificity of E-selectin. J. Biol. Chem. *270*, 14047–14055.

Kraulis, P.J. (1991). MOLSCRIPT: a program to produce both detailed and schematic plots of protein structure. J. Appl. Cryst. *24*, 946–950.

Lawrence, M.B., and Springer, T.A. (1991). Leukocytes roll on a selectin at physiologic flow rates: distinction from and prerequisite for adhesion through integrins. Cell *65*, 859–873.

Lee, T., Wisniewski, H.-G., and Vilcek, J. (1992). A novel secretory tumour necrosis factor-inducible protein (TSG-6) is a member of the family of hyaluronate binding proteins, closely related to the adhesion receptor CD44. J. Cell Biol. *116*, 545–557.

Lyon, M. (1986). Specific chemical modifications of link protein and their effect on binding to hyaluronate and cartilage proteoglycan. Biochim. Biophys. Acta *881*, 22–29.

Macura, S., Huang, Y., Sueter, D., and Ernst, R.R. (1981). Two-dimensional chemical-exchange and cross-relaxation spectroscopy of coupled nuclear spins. J. Magn. Reson. *43*, 259–281.

Maier, R., Wisniewski, H.-G., Vilcek, J., and Lotz, M. (1996). TSG-6 expression in human articular chondrocytes: possible implications in joint inflammation and cartilage degradation. Arthritis Rheum. *39*, 552–559.

Mikecz, K., Brennan, F.R., Kim, J.H., and Glant, T.T. (1995). Anti-CD44 treatment abrogates tissue oedema and leukocyte infiltration in murine arthritis. Nature Med. *1*, 558–563.

Morgelin, M., Paulsson, M., Hardingham, T.E., Heinegård, D., and Engel, J. (1988). Cartilage proteoglycans: assembly with hyaluronate and link protein as studied by electron microscopy. Biochem. J. *253*, 175–185.

Morgelin, M., Paulsson, M., Heinegård, D., Aebi, U., and Engel, J. (1995). Evidence of a defined spatial arrangement of hyaluronate in the central filament of cartilage proteoglycan aggregates. Biochem. J. *307*, 595–601.

Neame, P.J., and Barry, F.P. (1993). The link proteins. Experientia *49*, 393–402.

Neame, P.J., Christner, J.E., and Baker, J.R. (1986). The primary structure of Link protein from rat chondrosarcoma proteoglycan aggregate. J. Biol. Chem. *261*, 3519–3535.

Peach, R.J., Hollenbaugh, D., Stamenkovic, I., and Aruffo, A. (1993). Identification of hyaluronic acid binding sites in the extracellular domain of CD44. J. Cell Biol. *122*, 257–264.

Perkins, S.J., Nealis, A.S., Dudhia, J., and Hardingham, T.E. (1989). Immunoglobulin fold and tandem repeat structures in proteoglycan N-terminal domains and Link protein. J. Mol. Biol. *206*, 737–753.

Pouyani, T., and Prestwich, G.D. (1994). Biotinylated hyaluronic acid: a new tool for probing hyaluronate-receptor interactions. Bioconjug. Chem. *5*, 370–372.

Rauch, U., Karthikeyan, L., Maurel, P., Margolis, R.U., and Margolis, R.K. (1992). Cloning and primary structure of neurocan, a developmentally regulated, aggregating chondroitin sulfate proteoglycan of brain. J. Biol. Chem. *267*, 19536–19547.

Sharon, N. (1993). Lectin-carbohydrate complexes of plants and animal: an atomic view. Trends Biochem. Sci. *18*, 221–226.

Sheriff, S., Chang, C.-Y.Y., and Ezekowitz, R.A.B. (1994). Human mannose-binding protein carbohydrate recognition domain trimerizes through a triple α-helical coiled-coil. Struct. Biol. *1*, 789–794.

Sherman, L., Sleeman, J., Herrlich, P., and Ponta, H. (1994). Hyaluronate receptors: key players in growth, differentiation, migration and tumour progression. Curr. Opin. Cell Biol. *6*, 726–733.

Stein, P.E., Boodhoo, A., Armstrong, G.D., Cockle, S.A., Klein, M.H., and Read, R.J. (1994). The crystal structure of pertussis toxin. Structure *2*, 45–57.

Suri, A.K., and Levy, R.M. (1993). Estimation of interatomic distances in proteins from NOE spectra at longer mixing times using an empirical two-spin equation. J. Magn. Reson. *B101*, 320–324.

Underhill, C.B., Chi-Rosso, G., and Toole, B.P. (1983). Effects of detergent solubilization on the hyaluronate-binding protein from membranes of simian virus 40-transformed 3T3 cells. J. Biol. Chem. *258*, 8086–8091.

Varelas, J.B., Kollar, J., Huynh, T.D., and Hering, T.M. (1995). Expression and characterisation of a single recombinant proteoglycan tandem repeat domain of link protein that binds zinc and hyaluronate. Arch. Biochem. Biophys. *321*, 21–30.

Vyas, N.K. (1991). Atomic features of protein-carbohydrate interactions. Curr. Opin. Struct. Biol. *1*, 732–740.

Weis, W.I., Kahn, R., Fourme, R., Drickamer, K., and Hendrickson, W.A. (1991). Structure of the calcium-dependent lectin domain from a rat mannose-binding protein determined by MAD phasing. Science *254*, 1608–1615.

Weis, W.I., Drickamer, K., and Hendrickson, W.A. (1992). Structure of a C-type mannose-binding protein complexed with an oligosaccharide. Nature *360*, 127–134.

Wilmot, C.M., and Thornton, J.M. (1988). Analysis and prediction of different types of β-turns in proteins. J. Mol. Biol. *203*, 221–232.

Wisniewski, H.-G., Maier, R., Lotz, M., Lee, S., Lee, T.H., and Vilcek, J. (1993). TSG-6: a TNF-, IL-1-, and LPS-inducible secreted glycoprotein associated with arthritis. J. Immunol. *151*, 6593–6601.

Wisniewski, H.-G., Hua, J.-C., Poppers, D.M., Naime, D., Vilcek, J., and Cronstein, B.N. (1996). TNF/IL-1-inducible protein TSG-6 potentiates plasmin inhibition by inter-α-inhibitor and exerts a strong anti-inflammatory effect *in vivo*. J. Immunol. *156*, 1609–1615.

Yamada, H., Watanabe, K., Shimonaka, M., and Yamaguchi, Y. (1994). Molecular cloning of brevican, a novel brain proteoglycan of the aggrecan/versican family. J. Biol. Chem. *269*, 10119–10126.

Yang, B., Yang, B.L., Savani, R.C., and Turely, E.A. (1994). Identification of a common hyaluronan binding motif in the hyaluronan binding proteins RHAMM, CD44 and link protein. EMBO J. *13*, 286–296.

Yu, Q., and Toole, B.P. (1995). Biotinylated hyaluronan as a probe for detection of binding proteins in cells and tissue. Biotechniques *19*, 122–129.

Zheng, Z., Katoh, S., He, Q., Oritani, K., Miyake, K., Lesley, J., Hyman, R., Hamik, A., Parkhouse, R.M.E., Farr, A.G., and Kincade, P.W. (1995). Monoclonal antibodies to CD44 and their influence on hyaluronan recognition. J. Cell Biol. *130*, 485–495.

Zimmermann, D.R., and Ruoslahti, E. (1989). Multiple domains of the large fibroblast proteoglycan versican. EMBO J. *8*, 2975–2981.